# Evaluation of the difference-correction effect of the gamma camera systems used by easy Z-score Imaging System (eZIS) analysis

| メタデータ | 言語: eng |
|---|---|
| | 出版者: |
| | 公開日: 2017-10-03 |
| | キーワード (Ja): |
| | キーワード (En): |
| | 作成者: |
| | メールアドレス: |
| | 所属: |
| URL | http://hdl.handle.net/2297/36933 |

**Title Page**

**Type of article: original article**

**Evaluation of the difference correction effect of the gamma camera systems used**

**by easy Z-score Imaging System (eZIS) analysis.**

**Short title: Evaluation of difference correction effect of the camera used by eZIS**

・Yamamoto *et al.*

Yasushi Yamamoto[1,2], Masahisa Onoguchi[2], Kazunori Kawakami[3], Masuo Haramoto[1], Rei Wake[3], Jun Horiguchi[3], Hajime Kitagaki[4]

1) Department of Radiology, Shimane University Hospital
2) Department of Health Science, Graduate School of Medical Science, Kanazawa University
3) Department of Psychiatry, Shimane University School of Medicine
4) Department of Radiology, Shimane University Factory of Medicine

**Corresponding author**

Masahisa Onoguchi

Department of Health Sciences, Graduate School of Medical Sciences, Kanazawa University, Kodatsuno 5-11-80, Kanazawa, Ishikawa 920-0942, Japan

E-mail: onoguchi@staff.kanazawa-u.ac.jp

Phone & Fax: +81 76 265 2526

**Author**

Yasushi Yamamoto

Department of Radiology, Shimane University Hospital

89-1 Enya-cho, Izumo 693-8501, Shimane, Japan.

E-mail: yasushi@med.shimane-u.ac.jp

Phone : +81 853 20 2438

Fax : +81 853 20 2438

Kazunori Kawakami

Department of Psychiatry, Shimane University School of Medicine

89-1 Enya-cho, Izumo 693-8501, Shimane, Japan.

E-mail: kazunori@ffri.co.jp


Masuo Haramoto

Department of Radiology, Shimane University Hospital

89-1 Enya-cho, Izumo 693-8501, Shimane, Japan.

E-mail: haramoto@med.shimane-u.ac.jp


Rei Wake

Department of Psychiatry, Shimane University School of Medicine

89-1 Enya-cho, Izumo 693-8501, Shimane, Japan.

E-mail: rei@med.shimane-u.ac.jp


Jun Horiguchi

Department of Psychiatry, Shimane University School of Medicine

89-1 Enya-cho, Izumo 693-8501, Shimane, Japan.

E-mail: jhorigu@med.shimane-u.ac.jp


Hajime Kitagaki,

Department of Radiology, Shimane University Factory of Medicine

89-1 Enya-cho, Izumo, Shimane, Japan.

E-mail: kitagaki@med.shimane-u.ac.jp

1 ***Evaluation of the difference correction effect of the gamma camera systems used by***

2 ***easy Z-score Imaging System (eZIS) analysis***

3

4 **Abstract**

5 *Objective:* We examined the difference of the effect by data to revise a gamma camera

6 difference. The difference correction method of the camera is incorporated in eZIS

7 analysis.

8 *Methods:* We acquired SPECT data from the 3D Hoffman brain phantom (Hoffman),

9 the 3D brain phantom (3D brain), the Pool phantom (pool) and from normal subjects

10 (Normal-SPECT) to investigate compensating for a difference in gamma camera

11 systems. We compared SPECT counts of standard camera with the SPECT counts that

12 revised the difference of the gamma camera system (camera). Furthermore, we

13 compared the "Z-score map (Z-score)". In order to verify the effect of the compensation,

14 we examined digitally-simulated data designed to represent a patient with Alzheimer's

15 dementia. We carried out both eZIS analysis and "Specific Volume of interest Analysis

16 (SVA)".

17 *Results*: There was no great difference between the correction effect using Hoffman

18 phantom data and that using 3D-Brain phantom data. Furthermore, it was only over a

19 limited area that a good compensation effect was obtained. The compensation based

20 upon the Pool phantom was found to be the least satisfactory than other compensations

21 according to all result of a measurement examined in the study. The compensation based

22 upon the Normal-SPECT data resulted in a Z-score map (Z-score) for the result that

23 approximated that from the standard camera. Therefore, we concluded that the effect of

24 the compensation based upon Normal-SPECT data was the best of the four methods

1 tested.

2 *Conclusions:* Based upon eZIS analysis, the compensation using the Pool data was

3 inferior to the compensations using the other methods tested. Based upon the results of

4 the SAV analysis, the effect of the compensation using the Hoffman data was better than

5 the effect of the compensation using the 3D-Brain data. By all end-point measures, the

6 compensation based upon the Normal-SPECT data was more accurate than the

7 compensation based upon any of the other three phantoms.

8

9 *Keywords* $^{99m}$Tc-ECD • $^{99m}$Tc-HMPAO • SPM • eZIS • image compensation

10

11 **Introduction**

12

13 It has been reported that in the interpretation of cerebral blood flow images from

14 either positron emission tomography (PET) or single photon emission computed

15 tomography (SPECT), a diagnostic improvement is realized by statistical image analysis

16 using Statistical Parametric Mapping (SPM) [1, 2] or three-dimensional stereotactic

17 surface projections (3D-SSP) [3-5]. For the statistical image analysis, a normal database

18 (NDB) constructed from the images of a group of normal subjects is necessary. It is

19 used to make a reference image to which the image of a patient is compared [6-8].

20 Using a NDB constructed from one gamma camera system (camera) to analyze a patient

21 scan acquired on a different camera would appear to risk error because of differences in

22 the properties of the detectors and in the structure of the collimators used for different

23 cameras.

24 Using 3D-SSP, after a subject's brain image was aligned, spatially normalized into a

1    standard space, and smoothed, we measured counts from each pixel of the cerebral

2    surface for 6 pixels in the vertical direction of the cortex. We then extracted the

3    maximum count to the corresponding cerebral surface and performed imaging [9].

4    Therefore, the difference of the cameras and an anatomical error are thought to be

5    solved problems. Consequently, compensation for the difference in the cameras (the

6    camera which created the NDB and the camera which carried out the clinical study) is

7    not necessary [9].

8        In contrast, in the SPM analysis, the high-frequency component is removed by a

9    smoothing filter [10-11], and we were unable to employ the NDB if we did not

10   compensate for the difference in the cameras. Therefore, Matsuda et al. developed user

11   interface software that incorporated the difference correction method into the SPM2

12   analysis algorithm. It is the analytical method called easy Z-score Imaging System

13   (eZIS analysis) [5, 11-14].

14       Matsuda et al. also developed Alzheimer's dementia diagnosis support software called

15   Specific Volume of interest Analysis (SVA) [15-16]. SVA uses Voxel of interest (VOI)

16   of the disease specific region as a mask (SVA mask), and three diagnosis support indices

17   are calculated by regional Z-score. These indices are usually calculated after a

18   compensation for the difference in the cameras.

19       The difference compensation within the eZIS analysis functions as follows: First, we

20   collect Hoffman Brain phantom (Hoffman) data with the camera which created the

21   NDB and the camera which did the clinical study. Second, we multiply "Count Ratio" in

22   "Subjects data", and correct it so that it is as if the data were collected with the gamma

23   camera which created the NDB [11]. "Count Ratio" is the ratio of the Hoffman data that

24   we collected with the camera which we used for clinical studies and the Hoffman data

that we collected with the camera which created the NDB. Therefore, the eventual results of an analysis are thought to depend on the compensation effect (Correction effect of the camera difference). In an eZIS analysis, the Hoffman phantom is usually used to generate difference correction data. However, there have not been reports on the compensation effect when other phantoms are used.

**Objectives**

After having confirmed that a SPECT image varied according to a collector, we examined the difference of the correction effect by the data to revise a camera difference, in eZIS analysis. Also, we created data for difference corrections of the camera from the data of normal subject's, and examined it.

This study received the approval of the ethics committee of Shimane University School of Medicine.

**Materials and methods**

***The construction of the normal subjects' SPECT image data***

*The background of the normal subjects*

We recruited normal volunteers who did not suffer from brain disease and performed the cerebral blood flow SPECT examination using $^{99m}$Tc-ethyl cysteinate dimer ($^{99m}$Tc-ECD) on 20 subjects from March 2011 to September 2011. We recruited a

1    healthy volunteer to make normal database. And use it for making data to revise the

2    difference of the camera. The normal subject group consisted of 10 people in their 60s

3    (age 65.7 ± 2.2, 5 men, 5 women), and 10 people in their 70s (age 74.1 ± 2.2, 5 men, 5

4    women). The Hasegawa-style simple intelligence study (HDS-R) mean score was 28.5

5    ± 1.1 for those in their 60s, and was 28.4 ± 1.6 for those in their 70s. The Mini-Mental

6    State Examination (MMSE) mean score was 29.2 ± 1.7 for those in their 60s, and was

7    28.9 ± 1.7 for those in their 70s. It was necessary for us to know a subject's mean

8    cerebral blood flow (mCBF: ml/100g/min) to verify the normality of the brain blood

9    flow of people to be included in the normal database. We determined the mean cerebral

10    blood flow by the Patlak Plot method which is a noninvasive cerebral blood flow

11    measurement using non-blood sampling [17]. The mCBF was 43.4 ± 4.2 for those in

12    their 60s, and 41.8 ± 4.4 for those in their 70s.

13    We also recruited 32 other volunteers that were normal in their past brain health

14    examination that had been conducted to check for signs of cerebral infarctions

15    and other problems. These 32 volunteers were needed to allow one of the different

16    compensation methods and also for a NDB, as in the case with ^{99m}Tc-ECD. We acquired

17    cerebral blood flow SPECT images using ^{99m}Tc–hexamethylpropylene amine oxime

18    (^{99m}Tc-HMPAO) of these subjects from March 2010 to December 2010. The

19    normal-subject group was constructed of 10 people in their 50s (mean age 55.2 ± 3.0, 4

20    men, 6 women), 12 people in their 60s (mean age 63.8 ± 2.9, 7 men, 5 women), and 10

21    people in their 70s (mean age 73.2 ± 2.4, 5 men, 5 women). Okabe's Scale totals were

22    48.9 ± 3.0 for those in their 50s, 47.0 ± 5.7 for those in their 60s, and 45.4 ± 6.9 for

23    those in their 70s. The Okabe test is a modified and simplified version of the Wechsler

24    Memory Scale and consists of 4 subscales: information, mental control, digit span, and

1 associative learning. The full scores on these 4 subscales total 60 points. The

2 classification criteria are 10 points, severe dementia; 10～19 points, moderate dementia;

3 20～29 points, mild dementia (or notable mental aging) [18].

4     We again determined the mCBF by the Patlak Plot method; the mCBF was 47.3 ± 5.0

5 for those in their 50s, 43.4 ± 10.4 for those in their 60s, 41.7 ± 4.4 for those in their 70s.

6     In these two cases, there were no cases with abnormalities such as asymptomatic

7 cerebral infarction in MRI examination (MRI: signa HDX 3.0T and signa 1.5T, General

8 Electric), and the atrophy was suitable for their age.

9

10 *A SPECT image collection condition and the reconstruction parameters for normal*

11 *subjects*

12

13     We performed the cerebral blood flow SPECT examination using 740 MBq

14 of $^{99m}$Tc-ECD. The cameras used for imaging were a PRISM IRIX/Odyssey FX camera

15 / image processor (Philips Healthcare in Amsterdam, Netherlands) and an E.CAM/e.soft

16 camera/image processor (Siemens Healthcare in Munich, Germany). However, the

17 tracer was administered only once. Firstly, we collected SPECT data using the IRIX.

18 Less than 10 minutes elapsed after collection of the data with the IRIX before we started

19 to collect data with the E.CAM. The acquisition parameters with the IRIX camera:

20 energy window 140 keV ± 7.5%, and data sampling angle 5° step with 72 views (35

21 sec/view). A butterworth filter was used as a filtered back projection method for SPECT

22 image reconstruction at 0.75 cycle/cm. Attenuation compensation was performed using

23 Chang`s method with 0.1 cm$^{-1}$. That using E.CAM: camera, 140 keV ± 10%, 4° step /

24 90 views (15 sec/view), Butterworth filter 0.45 Nyquist frequency, Filtered Back

1 Projection, attenuation compensation by the Chang`s method with $0.1cm^{-1}$. The cut-off

2 frequency of the respective Butterworth filters had been set so that the resolution of the

3 image collected by one device was equal to the resolution of the image collected by the

4 other cameras [19]. Both cameras were equipped with low-energy high-resolution

5 collimators.

6     We performed another cerebral blood flow SPECT examination using 740 MBq

7 of $^{99m}$Tc-HMPAO. The SPECT image collection condition and reconstruction

8 parameters were the same as those for $^{99m}$Tc-ECD.

9

10 ***The acquisition and processing of phantom data to resolve the camera differences***

11 *(Fig.1)*

12

13     We used the Hoffman, the three-dimensional brain phantom (3D-Brain) and the Pool

14 phantom (Pool) data to construct the respective difference-compensation data. The

15 Hoffman differs from the human cranium and its brain because the phantom is

16 cylindrical and does not have an *ossa cranii*. To resolve these differences, Iida *et al.*

17 developed a phantom called the 3D-Brain. A bone equivalent fluid ($K_2HPO_4$) is

18 enclosed in the *ossa cranii* of the 3D-Brain. The cerebral parenchyma is constructed

19 from computed tomography (CT) images of normal subjects. A radioactive tracer can be

20 enclosed in the *substantia grisea* [20]. As for the Pool, brain parenchyma of Hoffman is

21 excluded; therefore the Pool is a simpler phantom than the Hoffman. We enclosed

22 0.3MBq/ml of $^{99m}$TcO4$^{-}$ in each phantom. We then acquired SPECT images with both

23 the IRIX camera and the E.CAM camera three times for each phantom. The SPECT

24 imaging conditions and image reconstruction conditions were the same as those for the

1    normal subjects. We performed anatomical standardization using a template suitable for

2    each phantom. The data for compensation were constructed from the average of the

3    three data sets.

4        In addition to using each of the three phantoms, we also used live subjects. That is,

5    we acquired images to resolve the differences between the two cameras from the

6    average of a set of normal-subject brain-blood-flow SPECT images. Furthermore, from

7    normal subject's average SPECT image data, we made data (Normal-SPECT data) for

8    difference compensation of the cameras. The procedure was to first realign the image,

9    and then anatomically standardize it using a template for ECD. And we made

10   Normal-SPECT data for both cameras (IRIX and E.CAM).

11       In the case of $^{99m}$Tc-HMPAO, we made compensation data (Normal SPECT data)

12   using 22 subjects (12 in their 60s and 10 in their 70s) average SPECT image data

13   similar to the case for $^{99m}$Tc-ECD.

14

15   ***The difference in SPECT image of the gamma cameras***

16

17       The data that we reconstituted from the normal subjects (n = 20) data that

18   used $^{99m}$Tc-ECD obtained with an E.CAM camera used it as reference data (Called in

19   what follows, "E.CAM Ref ECD data"). Similarly, that for the IRIX camera is called

20   "IRIX data". The procedure for producing what we called "E.CAM Ref ECD data" is

21   different from that for the above-mentioned "Normal-SPECT data". We collected the

22   raw data of normal subjects using the E.CAM and carried out attenuation correction and

23   reconstruction. We applied an anatomical standardization and smoothing. The result was

24   called the "E.CAM Ref ECD data" (n = 20). We used eZIS analysis (SPM2) for the

1    anatomical standardization and smoothing. We also collected normal subject raw data

2    with the IRIX and made IRIX data (n=20) in the same manner.

3        We performed a two-sample t-test (height threshold P value = 0.05, uncompensateed,

4    P value adjustments to none, extent threshold = 50 voxels) between the E.CAM Ref

5    ECD data and the IRIX data by the statistical mode of SPM8. The SPM8 software is the

6    current version of SPM. We thus assessed the difference in SPECT images (the

7    normalized SPECT counts) acquired by the two cameras. Hereinafter, in all two-sample

8    t-tests, we used the statistical mode of SPM8 and used the same procedure described

9    above.

10

11    ***Construction of data that artificially emphasizes the compensation effect.***

12

13        We reconstructed the raw data from the normal subjects acquired using the IRIX

14    without attenuation compensation (hereinafter referred to as IRIX AC⁻ data) in order to

15    clearly examine the effect of the compensation, that is, so that the relative difference in

16    count of the SPECT image data from the two cameras would be increased. We revised

17    the difference of the cameras for IRIX AC⁻ data. We calculate the count ratio of "Data

18    (there is attenuation compensation) to use for the difference compensation of the

19    cameras which we collected in E.CAM" and "Data (there is no attenuation

20    compensation) to use for the difference compensation of the cameras which we

21    collected in IRIX" every voxel. We multiplied every voxel of "IRIX AC⁻ data" in the

22    count ratio. We compared the E.CAM Ref ECD data with the IRIX AC⁻ data which

23    revised the difference of the cameras.

24

1 ***The evaluation of the effect of the compensation by the statistical significance test***

2 ***result images***

3

4     We constructed statistical significance test result images (hereinafter referred to as

5 "Decrease" and "Increase") by performing a two-sample t-test between the compensated

6 IRIX AC⁻ data and E.CAM Ref ECD data. In IRIX AC⁻ data, we did each compensation

7 methods "Hoffman data, 3D-Brain data, Pool data, Normal-SPECT data" and examined

8 an effect from "Decrease image" and "Increase image" as a reference E.CAM Ref ECD

9 data. The "Decrease image" shows those pixels where counts decreased in a statistically

10 significant way. The "Increase image" shows those pixels where counts increased in a

11 statistically significant way. We then visually examined the effect of the compensation.

12 Also, we compared IRIX AC⁻ data with E.CAM Ref ECD data.

13

14 ***The evaluation of the compensation effect by the Z-score***

15

16     We created a NDB (E.CAN NDB) using the normal subject raw data which we

17 collected using the E.CAM. We acquired a Z-score (map), which we define as a

18 standard Z-score map, by performing the eZIS analysis using the E.CAM NDB with the

19 E.CAM Ref ECD data. And we acquired a Z-score map by eZIS analysis using E.CAM

20 NDB with the compensated IRIX AC⁻ data. Also, we acquired the Z score (map) by an

21 eZIS analysis using E.CAM NDB with IRIX AC⁻ data to not compensate for the

22 difference of the camera. If the difference compensation is appropriate, the Z-score

23 should be similar to that of standard Z-score map. We calculated the average Z-score of

24 the "Decrease and Increase" for the central area (Fig. 3A) and for the marginal area (Fig.

1   3B) and evaluated the correction effect. We performed a multiple comparison by the

2   Tukey-Kramer method to test the statistical significance. A central area and the marginal

3   area divide a significant difference image which we made by two sample t-test between

4   E.CAM Ref ECD data and IRIX AC⁻ data into two regions. The division is made using

5   software for multipurpose image analyses named DRIP.

6

7   ***The evaluation of the correction by the correlation coefficient of the SPECT count***

8

9   We compensated IRIX data by multiplying the original IRIX data by the image of the

10   ratio of counts of difference-compensation data collected by E.CAM and constructed

11   with attenuation compensation (Hoffman data, 3D-Brain data, Pool data,

12   Normal-SPECT data) and counts of difference-compensation data collected by IRIX

13   and constructed with attenuation compensation. We calculated the correlation

14   coefficient of the SPECT count of "E.CAM Ref ECD data" and that of "Adjusted IRIX

15   data", and thereby evaluated a correction effect. That is we examined how similar the

16   Adjusted IRIX data was to E.CAM Ref ECD data.

17   Also, when we did not revise IRIX data, we examined it. The correlation coefficient

18   was calculated between every region of the same subjects. We set the regions using

19   Level 2 of "voxel-based Analysis Stereotactic Extraction Estimation (vbSEE)" [21]

20   which Mizumura developed; the six regions targeted for evaluation were: All Lobe,

21   Frontal Lobe, Occipital Lobe, Temporal Lobe, Anterior Lobe, Sub-lobar. (We calculated

22   right lobe and left lobe at one time). We used Matlab R2009b (MathWorks, Natick,

23   American MA state) for the calculation of the correlation coefficient. We used a

24   two-way factorial analysis of variance to test the statistical significance of the

Evaluation of difference correction effect of the camera used by eZIS

1 coefficient of correlation.

2

3 ***The construction of Alzheimer's dementia digital simulation data***

4

5     We constructed a SPECT image simulating Alzheimer's dementia for both cameras

6 (the IRIX AD and the E.CAM AD) from the SPECT images of a single subject (female,

7 63 years old, HDS-R:30 , MMSE:30). IRIX AD data and E.CAM AD decreased 20% of

8 SPECT counts of the SVA mask coordinate, and made it. This procedure was performed

9 by free software Daemon Research Image Processor. (DRIP: multipurpose image

10 analysis software, Fujifilm RI Pharma Ltd in Tokyo, Japan)

11

12 ***Compensation precision criterion by Z-score map where eZIS analyzed Alzheimer's***

13 ***dementia digital simulation data***

14

15 We corrected IRIX AD data, and performed eZIS analysis using E.CAM NDB, and

16 obtained a Z score map. Also, we made IRIX AD data without an attenuation

17 compensation, and acquired a Z score map by eZIS analysis using the E.CAM NDB. We

18 acquired a Z-score map by the eZIS analysis using IRIX NDB on IRIX AD data. We

19 acquired a Z-score map by the eZIS analysis using E.CAM NDB on E.CAM AD data.

20 We then visually examined these Z-score maps. We conducted SVA analysis, and

21 obtained Severity (Se), Extent (Ex) and Ratio. We compared each value, and evaluated a

22 correction effect. We can determine the "Extent" and "Severity" of the cerebral blood

23 flow drop by an SVA analysis. We can also determine the ratio of the brain blood flow

24 drop region over the whole brain by SVA analysis.

1

***Examination when healthy subject data group is different from a group constituting***

***Normal-SPECT data***

4

The effect of the compensation using Normal-SPECT data was assessed using the SPECT image data group of $^{99m}$Tc-HMPAO as the data group different from Normal-SPECT data constructing group. We performed a two-sample t-test between IRIX data using $^{99m}$Tc-HMPAO and the E.CAM Ref data using $^{99m}$Tc-HMPAO (hereinafter referred to as E.CAM Ref PAO data), between IRIX AC$^-$ data using $^{99m}$Tc-HMPAO and E.CAM Ref PAO data, and between "IRIX AC$^-$ data using $^{99m}$Tc-HMPAO that were compensated using Normal-SPECT data" and E.CAM Ref PAO data. We then constructed the statistical significance test result images and visually assessed the effect of the compensation for difference of cameras. E.CAM Ref PAO data, IRIX data of $^{99m}$Tc-HMPAO and IRIX AC$^-$ data of $^{99m}$Tc-HMPAO were constructed from the 10 normal subjects in their 50s belonging to the group that was not used for constructing Normal-SPECT data of $^{99m}$Tc-HMPAO for the compensation of the difference of cameras.

18

**Results**

20

***The difference in SPECT image of the gamma cameras***

22

Fig. 2A, show the results of the two-sample t-test between the E.CAM Ref ECD data and IRIX data of the normal-subject group. "Decrease" means the region in which the

1    counts of the IRIX data are lower than those of the E.CAM Ref data. "Increase" means

2    the region in which the counts of the IRIX data are higher than those of the E.CAM Ref

3    data. The counts of the IRIX data were lower than those of the E.CAM Ref ECD data in

4    the frontal lobe. Conversely, the counts of the IRIX data were higher than those of the

5    E.CAM Ref ECD data in the parietal lobe, temporal lobe and occipital lobe.

6

7    ***The evaluation of the effect of the compensation by the statistical significance test***

8    ***result images***

9

10      Fig. 2B, show the result of the two-sample t-test between E.CAM Ref ECD data and

11    IRIX AC$^-$ data. In the central area, the counts of the IRIX AC$^-$ data were significantly

12    lower than those of the E.CAM Ref ECD data. Conversely, in the marginal area, the

13    counts of the IRIX AC$^-$ data were significantly higher than those of the E.CAM Ref

14    ECD data. In Fig. 2C − F, we show the results of the two-sample t-test between the

15    E.CAM Ref ECD data and IRIX AC$^-$ data that were compensated by respective

16    difference-compensation data. "Increase image" is an image of the area that determined

17    that "IRIX AC$^-$ data which compensated the difference of the cameras" is bigger than

18    "E.CAM Ref ECD data". "Decrease image" is an image of the area that determined that

19    "IRIX AC$^-$ data which compensated the difference of the cameras" is smaller than

20    "E.CAM Ref ECD data". In the "Decrease image" of the central area, the difference in

21    count became less and visualized regions were decreased compared with the case

22    without the compensation (Fig. 2B). Hereby we confirmed the effect of the

23    compensation for difference of cameras. According to the "Increase image" (Fig. 2D),

24    which was compensated using 3D-Brain data, we confirmed that in the frontal lobe

1     there were the regions in which the difference in count increased compared with the

2     case without compensation.

3       From the visual assessment of the statistical significance test result images, it can be

4     seen that the difference in count was the smallest in the compensation using

5     Normal-SPECT data (Fig. 2F).

6

7     ***The evaluation of the compensation effect by the Z-score***

8

9       Fig.3 displays the Z-score of the central area of the Decrease and Increase images,

10     and that of the marginal area Decrease and Increase images. (The Z-score is on the

11     vertical axis). A horizontal axis, "IRIX data (No cor)" were case of the IRIX data that

12     does not correct the difference of the camera. "IRIX AC$^-$ data (No cor)" were case of the

13     IRIX AC$^-$ data that does not correct the difference of the camera. "E.CAM Ref ECD

14     data" was the case of the E.CAM Ref ECD data. "Hoffman data", "3D brain data",

15     "pool data" and "the normal SPECT data" were case of the adjusted IRIX AC$^-$ data

16     using each correction data. The NDB to use in all analyses is "E.CAM NDB".

17       Table.1 shows average and standard deviation (mean ± sd.) of Z-score. In the

18     Decrease side of the central area, Normal-SPECT data (0.7440 ± 0.190) and Hoffman

19     data (0.908 ± 0.168) did not have ECAM Ref ECD data (0.774 ± 0.218) and a

20     significant difference. In the "Decrease" of the central area, the most ineffective was the

21     compensation using 3D-Brain data (1.298 ± 0.160). Only Normal-SPECT data (-0.683 ±

22     0.129) did not have E.CAM Ref ECD data (-0.752 ± 0.122) and the significant

23     difference that was usual in the Increase side. Hoffman data (-1.245 ± 0.167) least had a

24     correction effect. In the marginal area, only Normal-SPECT data (0.741 ± 0.125, -0.833

1   ± 0.160) did not have a normal value and a significant difference with the Decrease side,

2   Increase side either. In Pool data (1.617 ± 0.133, 1.450 ± 0.191), the Decrease side of

3   the marginal area and the Increase side of the marginal area had no compensation effect.

4

5   ***The evaluation of the correction by the correlation coefficient of the SPECT count***

6

7   "IRIX data (No cor)" on the horizontal axis in Fig.4 were case of without the

8   compensation for the difference in cameras. "Hoffman data", "3D-Brain data", "Pool

9   data", "Normal-SPECT data" were case of corrected IRIX data that used each

10   correction data. The vertical axis shows the mean of correlation coefficient (Correlation

11   coefficient of each IRIX data SPECT counts and E.CAM Ref ECD data SPECT counts).

12   We show mean and standard deviation (mean ± sd.) of correlation coefficient in Table

13   2. In all regions, when we used Normal-SPECT data, the correlation coefficient was big

14   (0.963 ± 0.016). The correlation coefficient became smaller in order of IRIX data

15   (0.954±0.019), Hoffman data (0.942±0.025), 3D-Brain data (0.922±0.022), and Pool

16   data (0.917±0.023). We compared the correlation coefficient of every region. In

17   Occipital Lobe (0.963 ± 0.010) and Posterior Lobe (0.965 ± 0.011), the coefficient of

18   correlation is bigger than in other regions, and the standard deviation is small. In

19   Anterior Lobe (0.932 ± 0.027), Sub-lobar (0.926 ± 0.028), the coefficient of correlation

20   is smaller than for other regions, and the standard deviation is big. There was a

21   statistical significance between all difference-correction data. Furthermore, within type

22   of data set, there was a statistical significance between a value differences for all pairs

23   of regions.

24

1    *Compensation precision criteria by Z-score map where eZIS analyzed Alzheimer's*

2    *dementia digital simulation data*

3

4      In Fig. 5, we show the Z-score map of the IRIX AD data and that of E.CAM AD data

5    and the results of the SVA analysis. In order to reduce noise, the minimum threshold

6    value was set to 1.5. Fig. 5A shows the disease specific region which decreased the

7    SPECT counts (SVA mask) in white. Fig. 5B shows the Z-score map which analyzed

8    IRIX AD data in combination with the IRIX NDB. Fig. 5C shows the Z-score map

9    which analyzed E.CAM AD data in combination with the E.CAM NDB (standard

10    Z-score map). The Z-score map varied according to cameras. Fig. 5D shows Z-score

11    map which analyzed IRIX AD data which does not revise the difference of the cameras

12    in combination with the E.CAM NDB. The difference of the cameras compensates IRIX

13    AD data using Fig. 5E Hoffman data, Fig. 5F 3D-Brain data, Fig. 5G Pool data, Fig. 5H

14    Normal SPECT data and shows Z-score map which we analyzed in combination with

15    the E.CAM NDB. SVA analyzes each Z-score map and shows obtained Severity (Se),

16    Extent (Ex), Ratio in Fig. 5, lower section. The difference of the cameras compensates

17    IRIX AD data in "Hoffman data", "3D-Brain data", "Pool data", and Z-score map which

18    analyzed eZIS analysis has a bigger Z-score of the cerebellum region than standard

19    Z-score map, and Z-score of the posterior part of the cingulate gyrus is found to be

20    different. Z-score map which was the nearest to standard Z-score map was Z-score map

21    where the gap between the camera revised IRIX AD data in Normal-SPECT data (Fig.5

22    H). Without the compensation for the difference of the cameras (Fig. 5D), Z-score of the

23    cingulate gyrus rear than standard Z-score map was small, and the depicted range was

24    different.

1    The Z-score map which analyzed E.CAM AD data in combination with the E.CAM

2    NDB. Then, SVA analyzed, calculated Se, Ex and Ratio are standards of this

3    examination. Regarding the scores of the "Se" and "Ex", the most approximate

4    compensation to the standard of the present study (Fig. 5C: Se = 2.05, Ex= 47.08) was

5    the compensation using Normal-SPECT data (Se = 1.95, Ex =44.01). Followed in order

6    of the compensation using 3D-Brain data (Se = 1.93, Ex = 43.50), the compensation

7    using Hoffman data (Se = 1.79, Ex = 37.32), the compensation using Pool data (Se =

8    1.60, Ex = 29.07), no compensation (Se = 1.38, Ex = 20.68). Regarding the scores of

9    "Ratio", the most approximate compensation to the standard in the present study (Fig.

10    5C: 15.16) was the compensation using Hoffman data (17.30). When we did not revise

11    the difference of the cameras, the ratio was 18.45. When we used Normal-SPECT data

12    (31.06) for the difference compensation of the cameras, ratio showed a value larger than

13    a normal value. On the contrary, the "Ratio" of compensation using 3D-Brain data

14    (7.23) and that of compensation using Pool data (8.99) was lower than that of the

15    standard in the present study. Also, "Ratio" acquired by the analysis using IRIX NDB

16    on the IRIX AD data was 2.8 times higher than that of the standard in the present study.

17

18    ***Examination when healthy subject data group is different from a group constituting***

19    ***Normal-SPECT data***

20

21    Fig.6A, show the results of the two-sample t-test between the E.CAM Ref data

22    of ^{99m}Tc-HMPAO (hereinafter referred to as E.CAM Ref PAO data) and the IRIX data

23    of ^{99m}Tc-HMPAO. "Decrease" means the region in which the counts of IRIX data are

24    lower than those of the E.CAM Ref PAO data. And "Increase" means the region in

1   which the counts of the IRIX data are higher than those of the E.CAM Ref PAO data.

2   The counts of the IRIX data were lower than those of the E.CAM Ref PAO data in the

3   frontal lobe and higher than those of the E.CAM Ref PAO data in the parietal lobe,

4   temporal lobe and occipital lobe.

5     The counts of the IRIX AC⁻ data were significantly lower than those of the E.CAM

6   Ref PAO data in the central area and were significantly higher than those of the E.CAM

7   Ref data in the outside area (Fig.6B). Fig. 6C, show the results of the two-sample t-test

8   between IRIX AC⁻ data that were compensated using Normal-SPECT data and E.CAM

9   Ref PAO data. The difference in count of the "Decrease" in the central area and the

10   difference in count of the "Increase" in the outside area decreased. Therefore, the

11   difference compensation effect of the cameras is good.

12

13   **Discussion**

14

15     There was a statistical significance between the SPECT counts of the same subject

16   depending on the cameras. The statistical significance was not scattered, but occupied a

17   specific region such as the frontal lobe (Fig. 2A). Therefore, some compensation for the

18   difference of cameras is necessary to share an NDB in the eZIS analysis. If a result of

19   the eZIS analysis varies according to the difference of the device and cannot be

20   diagnosed definitely, this is because it is a problem.

21     In the present study, IRIX AC⁻ data approximated the E.CAM Ref ECD data because

22   of compensation. However, according to the examinations using the Hoffman by

23   Yamamoto [22] and Haramoto [23], a satisfactory effect of the compensation was not

24   achieved in all brain regions. In contrast, a satisfactory effect was achieved in the

1   compensation by Normal-SPECT data because the difference in count decreased in

2   "Decrease image" and "Increase image". A stable compensation effect was provided in

3   Central area and outside area. By the compensation using Phantom data including

4   Hoffman, it has the area where a good compensation effect is not provided.

5     The above result was also proven by the assessment of the effect of the compensation

6   by Z-score (Fig. 3 and Table 1). A satisfactory effect of the compensation could be

7   achieved only in compensation using Normal-SPECT data in both the central area and

8   the marginal area. In the compensations using the other phantom data, the central area

9   was inconsistent with the marginal area and "Decrease" was inconsistent with

10   "Increase". This is due to the difference of the formulations distribution, which arose

11   from the difference in structure between the phantom data and actual brain tissue

12   because the image reconstruction conditions were set so that the resolutions were the

13   same in each SPECT image of the two cameras [19]. The Z-score acquired by eZIS

14   analysis using the E.CAM NDB on the IRIX data without compensation, IRIX data (No

15   cor), was more approximate to the standard Z-score than the compensation using

16   Phantom data. Therefore, although the cameras differed, if we equalize the image

17   reconstruction conditions of the collection camera and those of the standard camera (the

18   NDB constructing camera), we were able to acquire data that better approximated the

19   E.CAM Ref ECD data than the data acquired by the compensation for difference of

20   cameras using phantom data.

21     Fig.4 and Table.2, show the results of the assessment of correction effect of

22   compensation by the correlation coefficient of SPECT counts, the correlation coefficient

23   between the E.CAM Ref ECD data and IRIX data (No cor) were higher than the

24   correlation coefficient between the E.CAM Ref ECD data and IRIX data compensated

Evaluation of difference correction effect of the camera used by eZIS

1    by phantom data. Suggested by the examination using Z-score as mentioned above,

2    equalizing the image reconstruction conditions of the collection camera and those of the

3    standard camera (the NDB constructing camera) is more effective than the

4    compensation of the difference of the cameras using phantom data. We do not do the

5    difference compensation of the cameras, but use the NDB.

6      The effect of the compensation using Normal-SPECT data was satisfactory because

7    the correlation coefficients were the highest in all regions. On the contrary, the

8    correlation coefficients of the compensation using Pool data were the lowest in all

9    regions except for the Sub-Lobar. Among these regions, in the anterior lobe, the

10    correlation coefficient was especially low. The anterior lobe was the region in which the

11    difference in count was large in the compensation by Pool data (Fig.2E). This meant

12    that the effect of the compensation by Pool data was found to be restrictive.

13      The eZIS analyzed E.CAM AD data in combination with the E.CAM NDB. Then, we

14    performed SVA analysis. And calculated "Se and Ex" are standards. Se and Ex of the

15    compensation using 3D-Brain data (Fig.5F) were the most approximate to the standard

16    among those of the compensations using Pool data. However, the Ratio was the smallest

17    among all compensations. This meant the existence of many voxels with Z-score$\geqq 2$

18    produced by the compensation in the Z-score map. Therefore, the 3D-Brain data were

19    not appropriate data for the compensation. Similarly, in the compensations using Pool

20    data, Ratios were small; therefore, Pool data were not appropriate data for compensation.

21    In the compensation using Hoffman data (Fig.5E), Se and Ex were approximate to the

22    standard scores. This result was more satisfactory than the case of no compensation

23    (Fig.5D). For the reasons stated above and the result of SVA analysis, among three

24    Phantom data, only Hoffman data were appropriate for the compensation. We are

1  satisfied with the result of the SVA analysis, but are not satisfied with the result of the

2  eZIS analysis. If we use it for difference compensation of the cameras by Phantom data,

3  we think that it is Hoffman data.

4     3D-Brain is the phantom which best simulated the brain of humans, but only the gray

5  matter area that we can contain a radionuclide. On the other hand, Hoffman employs a

6  gap between the plates of the 89 slices but allows for a white matter area and a gray

7  matter area. We infer that it is nearer to the distribution of the brain of humans. In other

8  words the thing more necessary for compensation is distribution rather than perfect

9  structure.

10      In Fig. 6A, we show the differences in the SPECT image due to the camera in the

11  case of $^{99m}$Tc-HMPAO. The "Decrease" image and "Increase" image in the case

12  of $^{99m}$Tc-HMPAO showed the same tendency as in the case of $^{99m}$Tc-ECD (Fig. 2A). It

13  has been reported that both $^{99m}$Tc-HMPAO distributions and $^{99m}$Tc-ECD distributions in

14  the brain are the same a few hours after administration [24-28]. Therefore, this

15  statistical significance clearly shows the differences in the SPECT image by the camera.

16  When we use Normal-SPECT data for the difference compensation of the cameras:

17  When radiopharmaceutical compares the case of $^{99m}$Tc-HMPAO (Fig.6C) and the case

18  of $^{99m}$Tc-ECD (Fig. 2F), in the case of $^{99m}$Tc-HMPAO, the regions with significant

19  differences were mostly scattered throughout the brain. On the other hand, the statistical

20  significance of the central area (Fig. 6B) disappeared; therefore we were able to obtain a

21  satisfactory compensation effect. However, for the compensation using Normal-SPECT

22  data, we must collect the same normal subject's raw data by both the camera which

23  created the NDB and the camera used for the clinical study. This procedure is more

24  difficult than constructing an NDB.

1    Therefore, in future work, we will study the ways to conveniently construct the data

2    for the compensation of the difference of collection camera by extracting a control

3    group from the clinical data obtained with each camera. This control group should

4    consist of over 25 cases, which are regarded as a large sample.

5

6    **Conclusions**

7

8    We verified differences in SPECT images of cerebral blood flow caused by a

9    difference in the imaging camera. It was what had been already checked, but we

10   inspected it. There was a difference in the frontal lobe, parietal lobe, temporal lobe, and

11   occipital lobe when we compared the SPECT image of E.CAM with the SPECT image

12   of the IRIX. The difference compensation of the cameras using Pool data in the eZIS

13   analysis was not able to confirm the good compensation effect in all end-points that we

14   examined in this study. The excellent compensation was achieved by using Hoffman

15   data rather than 3D-Brain data. The effect of the difference compensation of the cameras

16   using Normal - SPECT data was superior to the compensation effect using each of the

17   three Phantom data sets.

18

19   **References**

20

21   1. Friston KJ, Holmes AP, Worsley KJ, poline J-P, Frith CD, Frackowiak RSS, et al.

22      Spatial registration and normalization of image. Human Brain Mapping 1995 ; 2 :

23      165-189.

24   2. Friston KJ, Holmes AP, Worsley KJ, poline J-P, Frith CD, Frackowiak RSS, et al.

1    Statistical parametric maps in functional imaging : a general linear approach. Human

2    Brain Mapping 1995 ; 2 : 189-210.

3    3. Minoshima S, Foster NL, Kuhl DE. Posterior cingulate cortex in Alzheimer's disease.

4    Lancet. 1994 Sep 24; 344 (8926): 895.

5    4. Minoshima S, Frey KA, Koeppe RA, Foster NL, Kuhl DE. A diagnostic approach in

6    Alzheimer's disease using three-dimensional stereotactic surface projections of

7    fluorine-18-FDG PET. J Nucl Med. 1995 Jul; 36 (7):1238-48.

8    5. Yamamoto Y, Onoguchi M. Statistical image analysis in the cerebral Blood Flow

9    SPECTW'A difference and matters that require attention of the handling of eZIS and

10   iSSP. Nippon Hoshasen Gijutu Gakkai Zashi. 2011; 67(6): 719-27.

11   6. Matsuda H, Mizumura S, Nagao T, Ota T, Iizuka T, Nemoto K, et al. An easy Z-score

12   imaging system for discrimination between very early Alzheimer's disease and

13   controls using brain perfusion SPECT in a multicenter study. Nucl Med Commun.

14   2007 Mar;28(3):199-205.

15   7. Ishii K, Kono AK, Sasaki H, Miyamoto N, Fukuda T, Sakamoto S, et al. Fully

16   automatic diagnostic system for early- and late-onset mild Alzheimer's disease using

17   FDG PET and 3D-SSP. Eur J Nucl Med Mol Imaging. 2006 May; 33(5): 575-83.

18   8. Ishii K, Kanda T, Uemura T, Miyamoto N, Yoshikawa T, Shimada K, et al.

19   Computer-assisted diagnostic system for neurodegenerative dementia using brain

20   SPECT and 3D-SSP. Eur J Nucl Med Mol Imaging. 2009 May; 36(5): 831-40.

21   9. Imabayashi E. 3D-SSP: Principle and modality of image statistical analysis. In:

22   Matsuda H, Asada T. Imaging of dementia. Tokyo: Nagai Bookstore Co, Ltd;   2004

23   p. 92-94.

24   10. Oonishi T. SPM: Principle and modality of image statistical analysis. In: Matsuda H,

1    Asada T. Imaging of dementia. Tokyo: Nagai Bookstore Co, Ltd; 2004 p. 82-83.

2    11. Yamamoto Y. The basics of Easy Z-score Imaging System: Kawamura S, Yamamoto

3    T. Base and application of the clinical analysis software in nuclear medicine. Tokyo:

4    Nippon Hoshasen Gijiutu Gakkai publication committee; 2011 p. 1-7.

5    12. Matsuda H, Mizumura S, Soma T, Takemura N. Conversion of brain SPECT images

6    between different collimators and reconstruction processes for analysis using

7    statistical parametric mapping. Nucl Med Commun. 2004 Jan;25(1):67-74.

8    13. Mizumura S, Kumita S. Stereotactic statistical imaging analysis of the brain using

9    the easy Z-score imaging system for sharing a normal database. Radiat Med. 2006

10   Aug; 24(7): 545-52.

11   14. Hiroshi M. eZIS: Principle and modality of image statistical analysis. In: Matsuda H,

12   Asada T. Imaging of dementia .Tokyo: Nagai Bookstore Co, Ltd; 2004 p. 96-102.

13   15. Matsuda H, Mizumura S, Nagao T, Ota T, Iizuka T, Nemoto K, et al. Automated

14   discrimination between very early Alzheimer disease and controls using an easy

15   Z-score imaging system for multicenter brain perfusion single-photon emission

16   tomography. AJNR Am J Neuroradiol. 2007 Apr; 28(4): 731-6.

17   16. Yamamoto Y. The clinical use of Specific VOI analysis (SVA): Kawamura S,

18   Yamamoto T. Base and application of the clinical analysis software in nuclear

19   medicine .Tokyo: Nippon Hoshasen Gijiutu Gakkai publication committee; 2011 p.

20   23-28.

21   17. Matsuda H., Tsuji S, Shuke N, Sumiya H, Tonami M, Hisada K. A quantitative

22   approach to technetium-99m hexamethylpropylene amine oxime. Eur J Nucl

23   Med.1992; 19(3): 195-200.

24   18. Kobayashi S, Yamaguchi S, Kitani M, Okuda K, Shimote K. Evaluation of practical

usefulness of the Okabe's mini-mental scale in normal aged. Japanese Journal of Neuropsychology. 1987; 3: 67-72.

19. Yamamoto Y, Haramoto M, Komatsu A, Kurihara H. A study of normal data base in 3D-SSP. Nippon Hoshasen Gijiutu Gakkai Zashi. 2005; 61(4): 529-36 (in Japanese).

20. Iida H, Hori Y, Ishida K, Tsushima H, Imabayashi E, Matsuda H, Takahashi M, et al. Tree-dimensional brain phantom containing bone and grey matter structures with a realistic heah contour. Ann Nucl Med. 2013; 27(1): 25-36.

21. Mizumura S. Affiliation symptom diagnosis using a function image and a configuration image. Image integration of VSRAD and eZIS/SPM. Rounen   Seishin Igaku Zashi. [A commentary / special feature]. 2008; 19 (An extra number I): 41-51.

22. Yamamoto Y, Oonishi H, Murakami T, Takahashi M, Odajima S, Uchida K. Research Report: accuracy and evaluation of the stereotactic statistical imaging analysis of the brain. Nippon Hoshasen Gijutu Gakkai Zashi. 2008; 64(6): 752-65.

23. Haramoto M, Yamamoto Y, Akio K. Fundamental examination of eZIS. Nippon Hoshasen Gishikai Zashi. 2006; 53(1): 26-33.

24. Matsuda H, Terada H, Higashi S, Sumiya H, Tsuji S, Seki H, et al. Basic and Clinical Studies of Brain Perfusion Scintigraphy Using 99mTc-d,l-hexamethyl-propyleneamine Oxime. Kaku Igaku.1987.09; 24(9): 1329-41.

25. Tukamoto E, Itoh K, Kamiyama H, Mabuchi S, Furudate M. Clinical Experience of 99mTc-hexamethylpropyleneamine Oxime(99mTc-HMPAO) for Imaging of Regional Cerebral Blood Flow. Kaku Igaku.1987.10; 24(10): 1573-9.

26. Yokota I, Oka H, Ogura H, Hayashi M. Basic and Clinical Evaluation of Cerebral Blood Flow Scintigraphy with Tc-99m d,1-HM-PAO. Nippon Hoshasen Gijutu

1    Gakkai Zashi.1988. 07; 44(7): 750-8.

2    27. Matsuda H, Kinuya K, Higashi S, Kawasaki Y, Sumiya H, Shuke N, et al.

3    Evaluation of Perfusion SPECT Imaging Using 99mTc-ECD. Kaku Igaku.1991.07;

4    28(7): 701-9.

5    28. Ichise M, Golan H, Ballinger JR, Vines D, Blackman A, Moldofsky H. Regional

6    differences in technetium-99m-ECD clearance on brain SPECT in healthy subjects. J

7    Nucl Med. 1997; 38(8): 1253-60.

8

1    **Figure Legends**

2

3    **Figure 1**

4    Photographs of three phantoms and its images. A Hoffman phantom and its CT image

5    (A). A 3D-Brain phantom and its CT image (B). A pool phantom (C). All of four images

6    below show the SPECT image for compensations that were obtained by the IRIX

7    camera. The Hoffman data (D), the 3D-Brain data (E), the Pool data (F), and the

8    Normal-SPECT data (G).

9

10    **Figure 2**

11    Maximum intensity projection (MIP) of SPM8 result for each two-sample t-tests on

12    basis of E.CAM Ref ECD data by $^{99m}$Tc-ECD SPECT. MIPs show the increase and

13    decrease for IRIX data (A), IRIX AC$^{-}$ data (B), compensated IRIX AC$^{-}$ data by

14    Hoffman (C), compensated IRIX AC$^{-}$ data by 3D-Brain (D), compensated IRIX AC$^{-}$

15    data by Pool (E) and compensated IRIX AC$^{-}$ data by Normal-SPECT (F), respectively.

16

17    **Figure 3**

18    The binarized images of Fig.2 (B) show the Central (A) and Marginal (B). The Z-score

19    below shows both increase and decrease that analyzed by each compensation methods.

20    Each polygonal line of the Z-score corresponds to the same subjects.

21    ＊ n.s.(P≥0.05).

22

23    **Table 1**

24    The average and the standard deviation (mean ± SD) of the Z-scores in central area (A)

1    and marginal area (B) analyzed by each compensation methods.

2

3    **Figure 4**

4    The correlation coefficient of the Z-scores by each compensation methods using vbSEE

5      (Level 2) that simultaneously analyzed of both right lobe and left lobe. Each polygonal

6      line of the each compensation methods corresponds to the same subjects.

7

8    **Table 2**

9    The average and the standard deviation (mean ± SD) of the correlation coefficients

10    between Z-scores and each compensation methods on the basis of E.CAM Ref ECD

11    data. All areas were automatically-divided by vbSEE.

12

13    **Figure 5**

14    The above images show the Z-score map calculated by the eZIS analysis. The

15    simulation image (A) which made intentionally-decreased of the SPECT counts using

16    SVA mask processing (as white) for the disease specific regions in order to simulate the

17    AD. Others are the Z-score map images for IRIX AD data using IRIX NDB (B),

18    E.CAM AD data using E.CAM NDB (C), IRIX AD data using E.CAM NDB (D),

19    compensated IRIX AD data by Hoffman data using E.CAM NDB (E), compensated

20    IRIX AD data by 3D-Brain data using E.CAM NDB (F), compensated IRIX AD data by

21    Pool data using E.CAM NDB (G), compensated IRIX AD data by Normal SPECT data

22    using E.CAM NDB (H). Table below shows the index values (Severity, Extent and

23    Ratio) analyzed by SVA from Z-score map.

24

1     **Figure 6**

2     Maximum intensity projection (MIP) of SPM8 result for each two-sample t-tests on

3     basis of E.CAM Ref PAO data by ^{99m}Tc-HMPAO SPECT. MIPs show the increase and

4     decrease for IRIX data (A), IRIX AC[-] data (B), compensated IRIX AC[-] data by

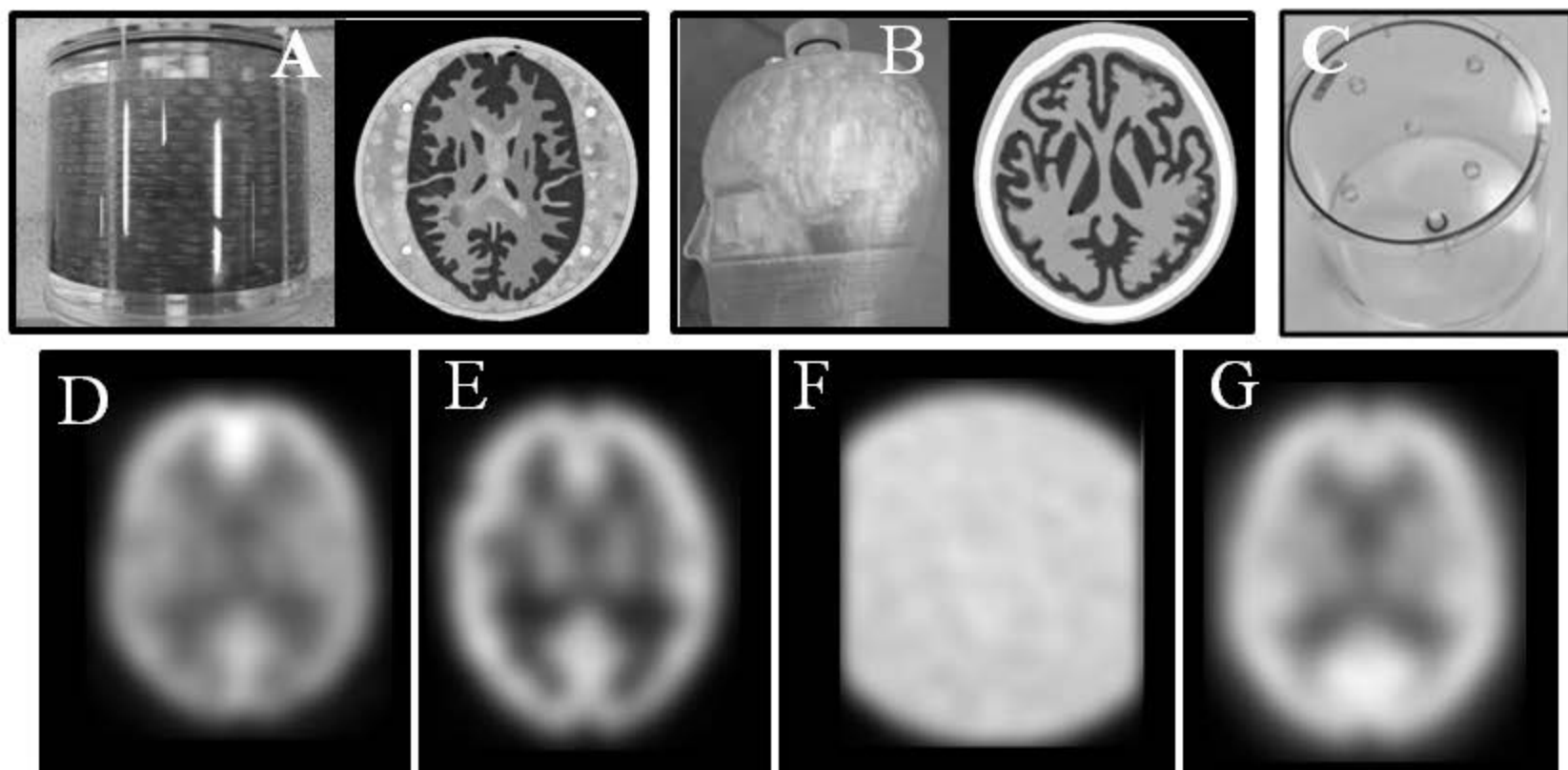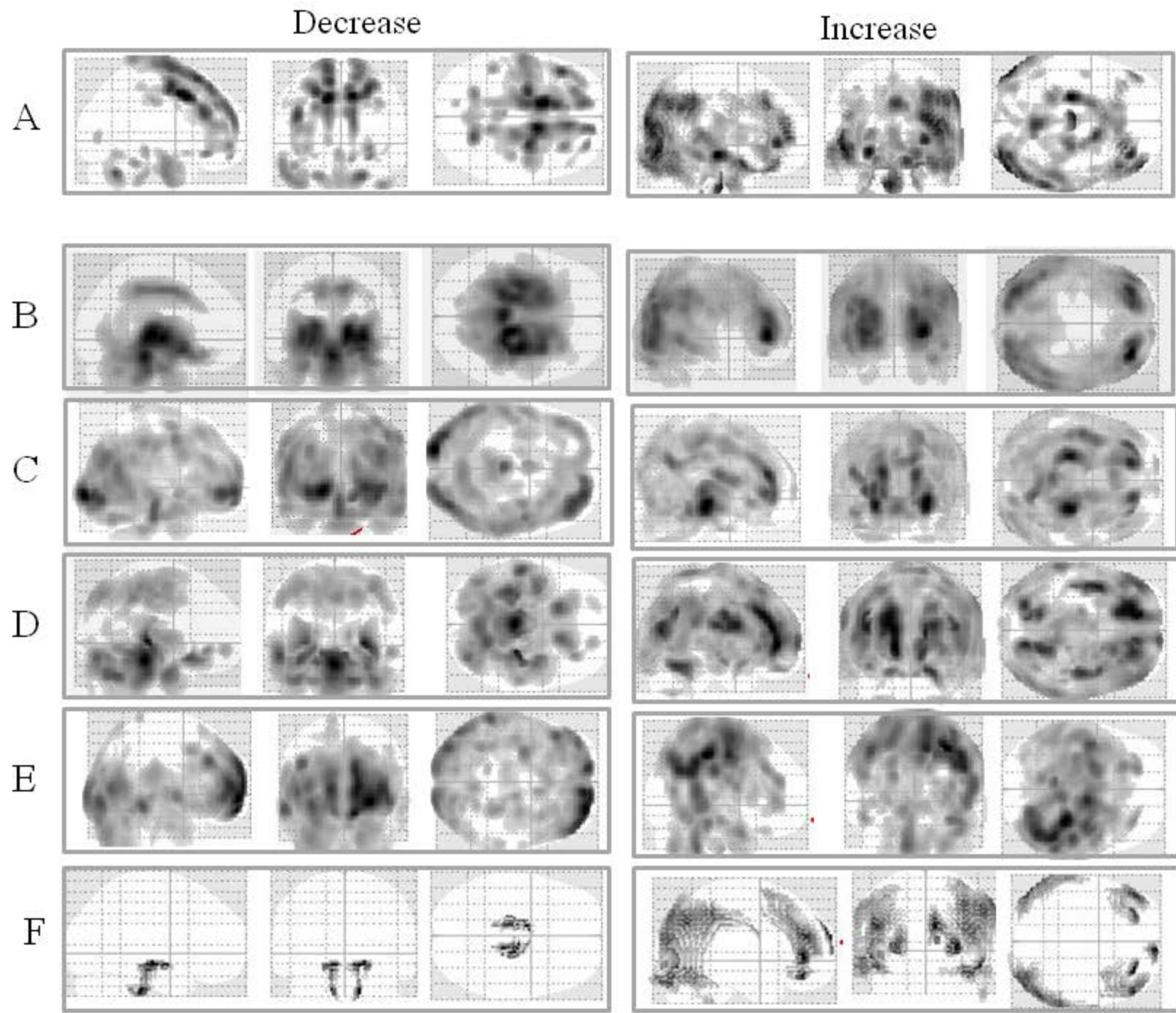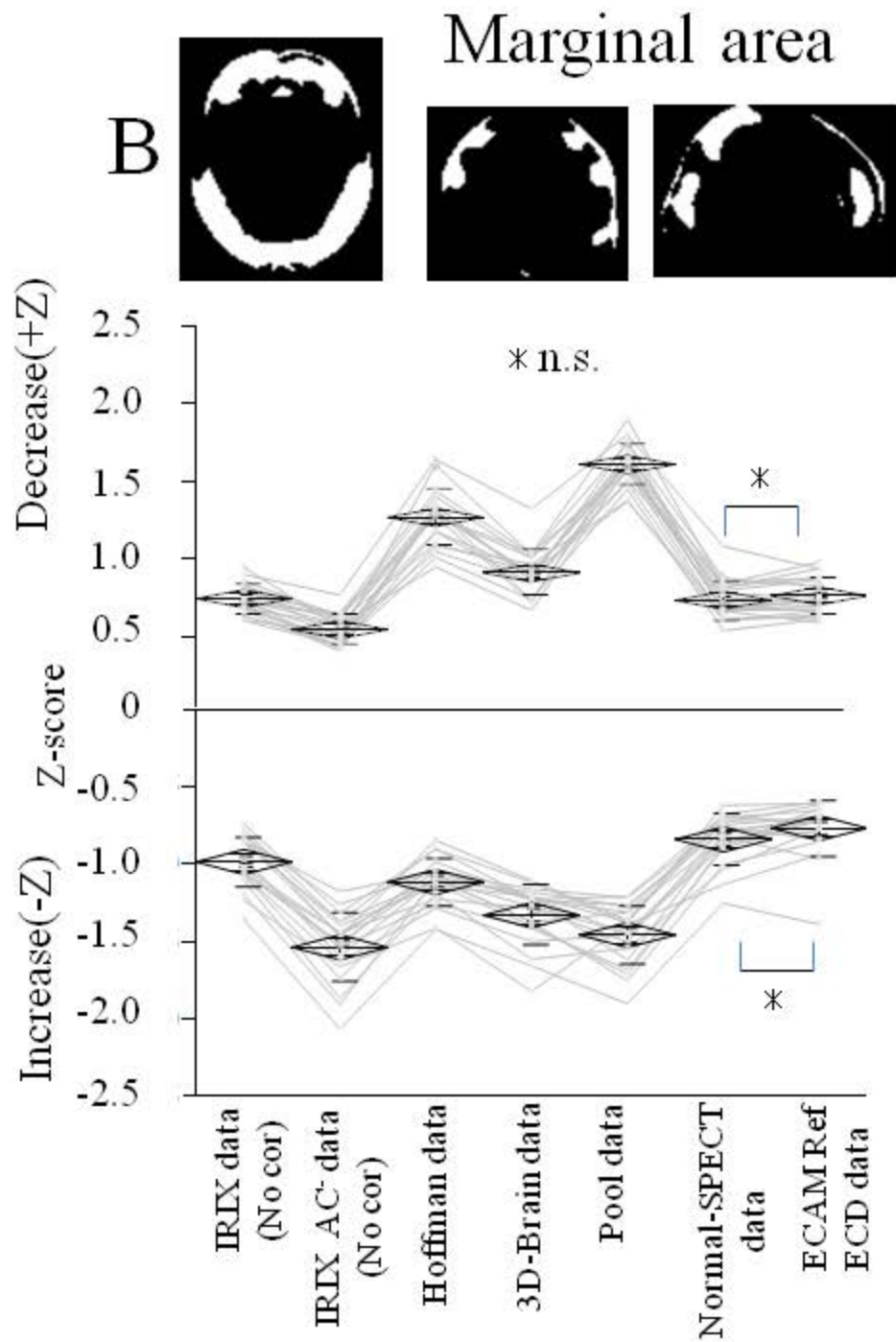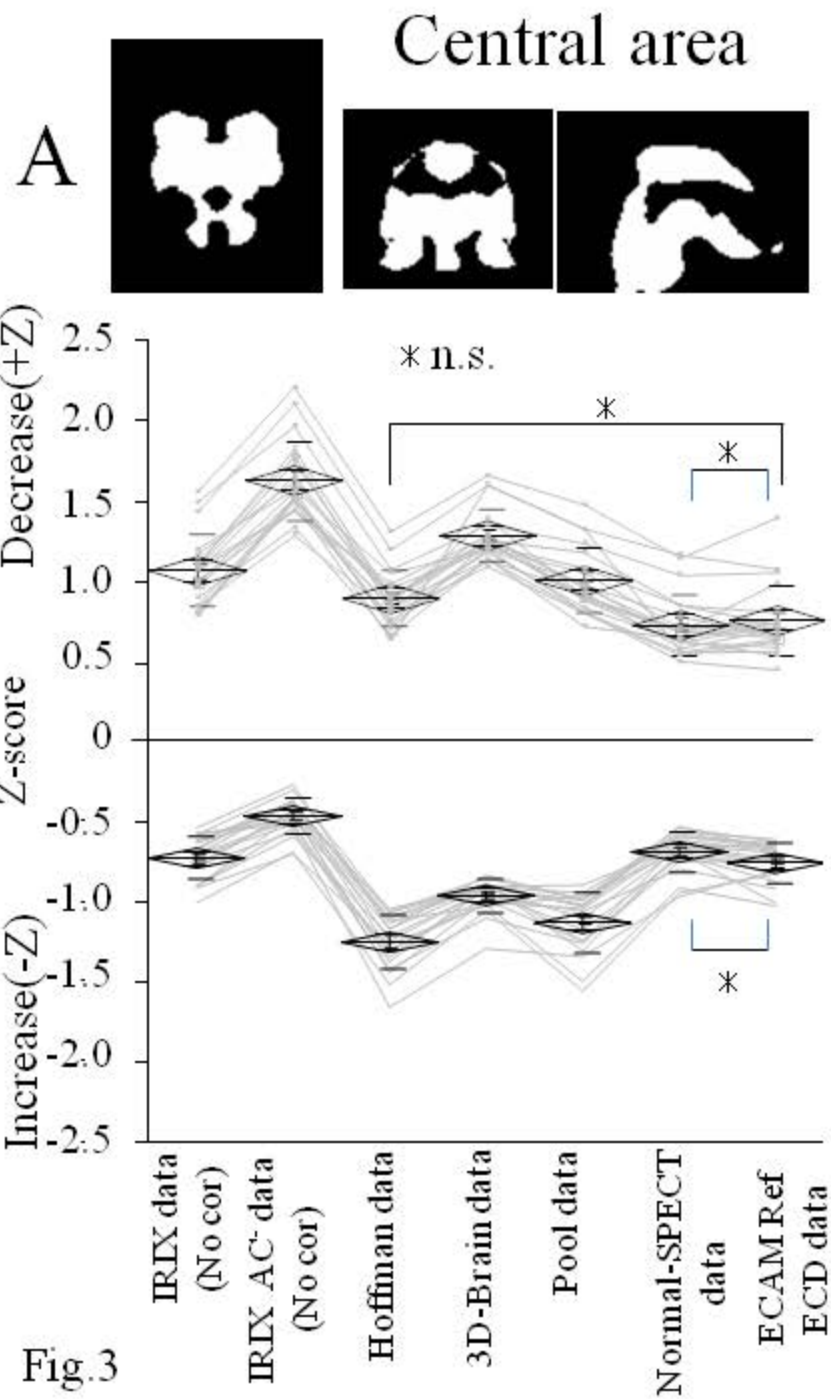5     Normal-SPECT (C), respectively.

Fig.1

| Decrease | Increase |
|---|---|

A

B

C

D

E

F

Fig.2

Fig.3
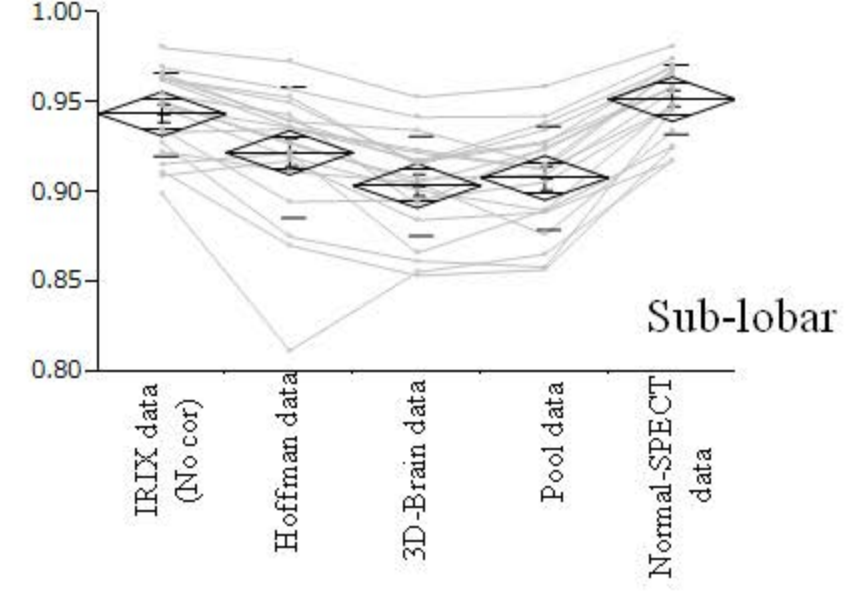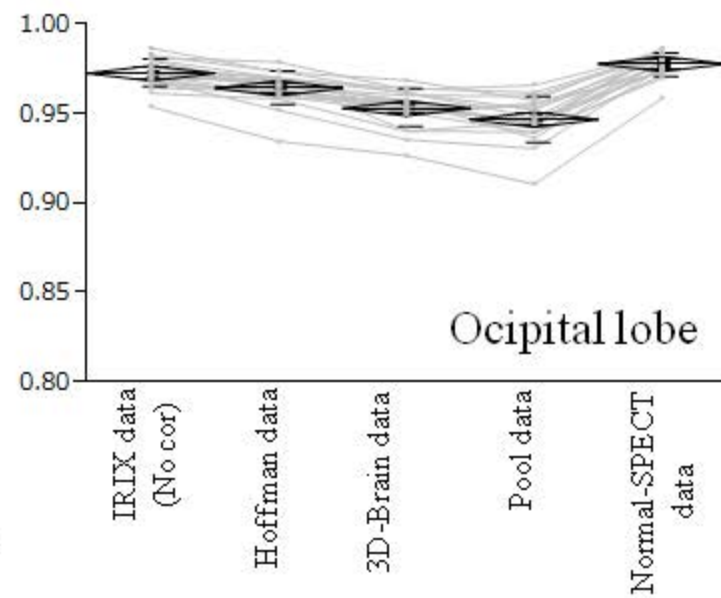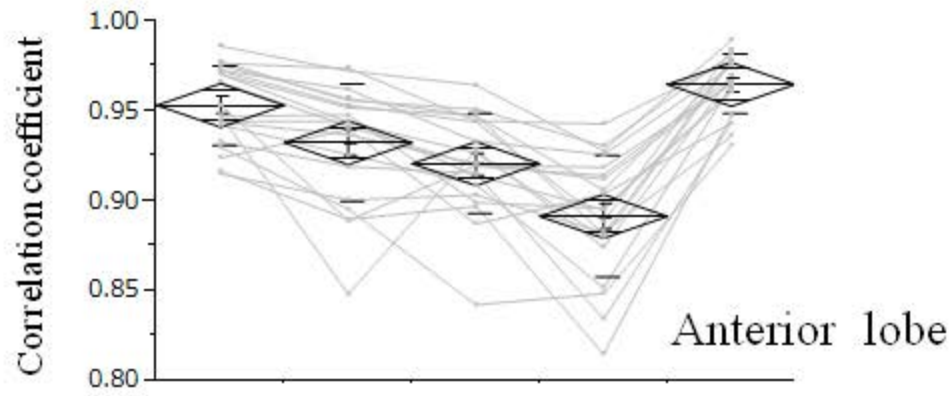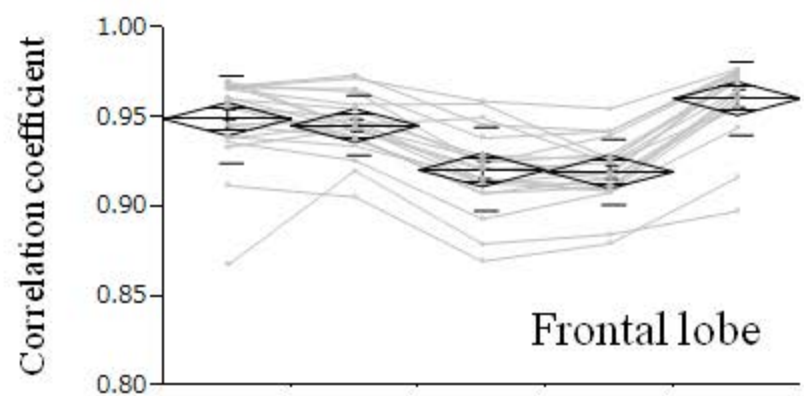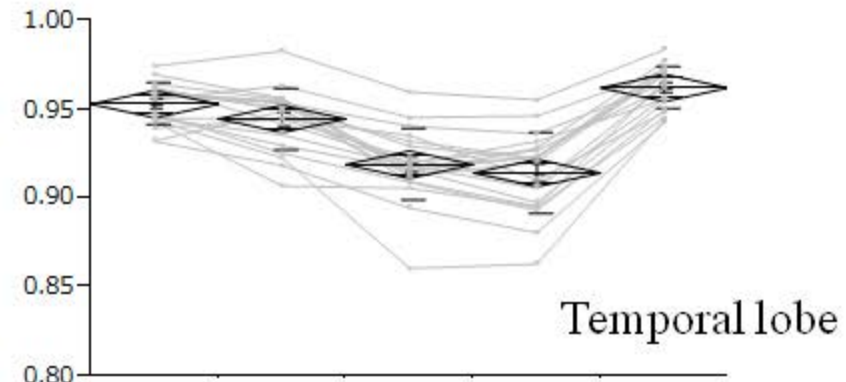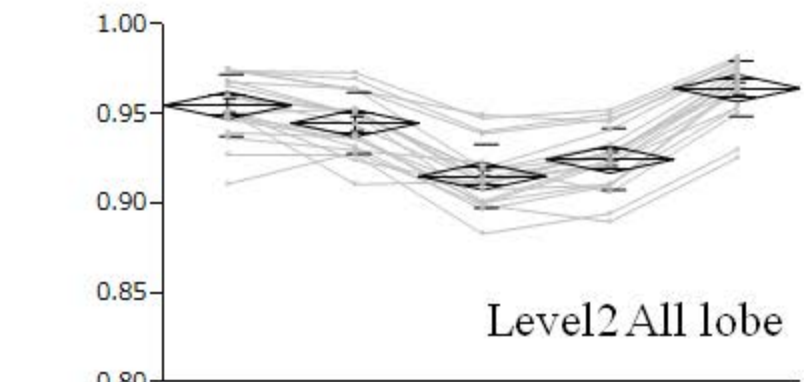
Fig.4
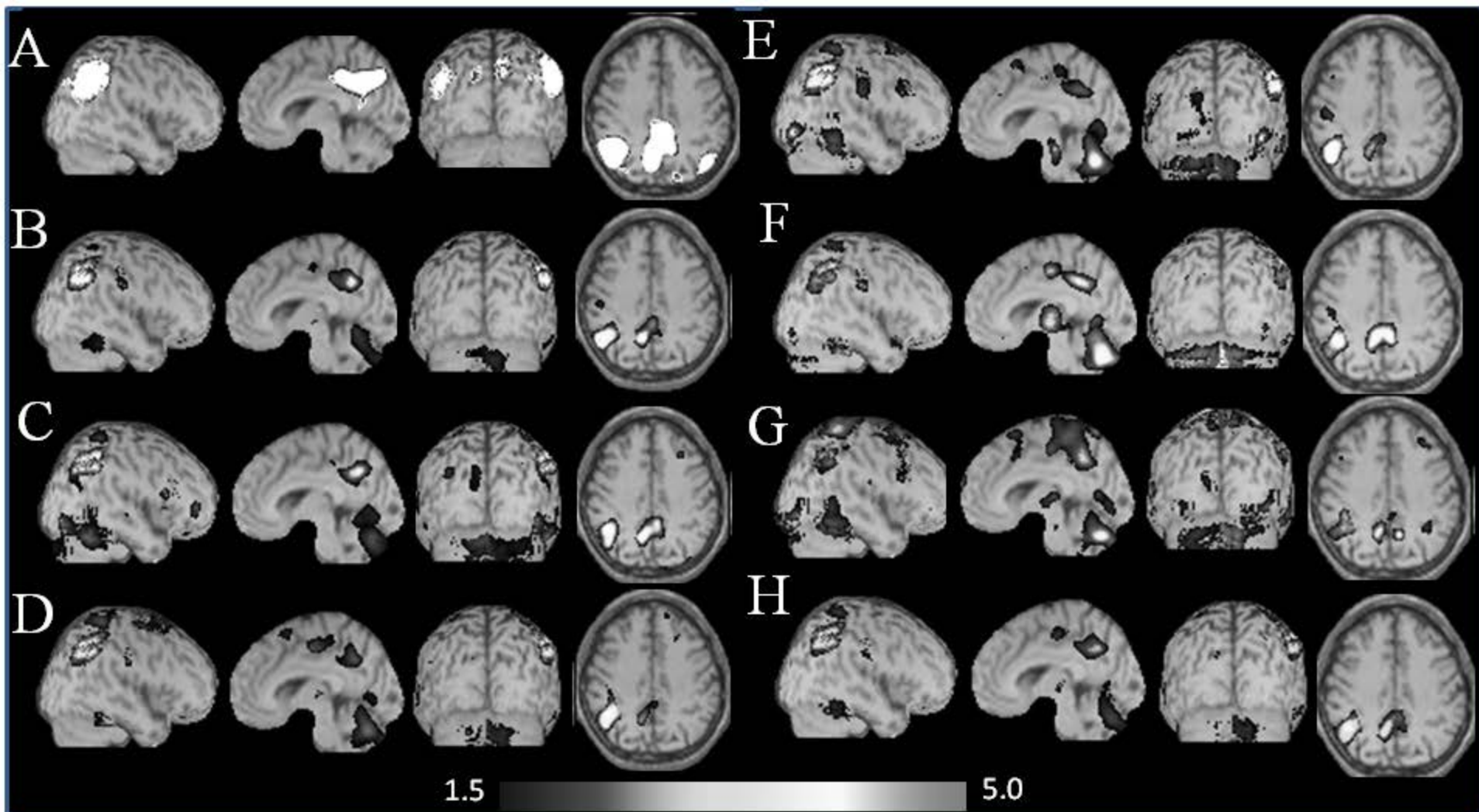
| | Severity | Extent | Ratio |
|---|---|---|---|
| B: IRIX AD data with IRIX NDB | 1.67 | 32.98 | 42.66 |
| C: ECAM AD data with ECAM NDB | 2.05 | 47.08 | 15.16 |
| D: IRIX AD data with ECAM NDB (No cor) | 1.38 | 20.68 | 18.45 |

| | Severity | Extent | Ratio |
|---|---|---|---|
| E: Hoffman data | 1.79 | 37.32 | 17.30 |
| F: 3D-Brain data | 1.93 | 43.50 | 7.23 |
| G: Pool data | 1.60 | 29.07 | 8.99 |
| H: Normal-SPECT data | 1.95 | 44.01 | 31.06 |

Fig.5

Decrease                                    Increase

A

B

C
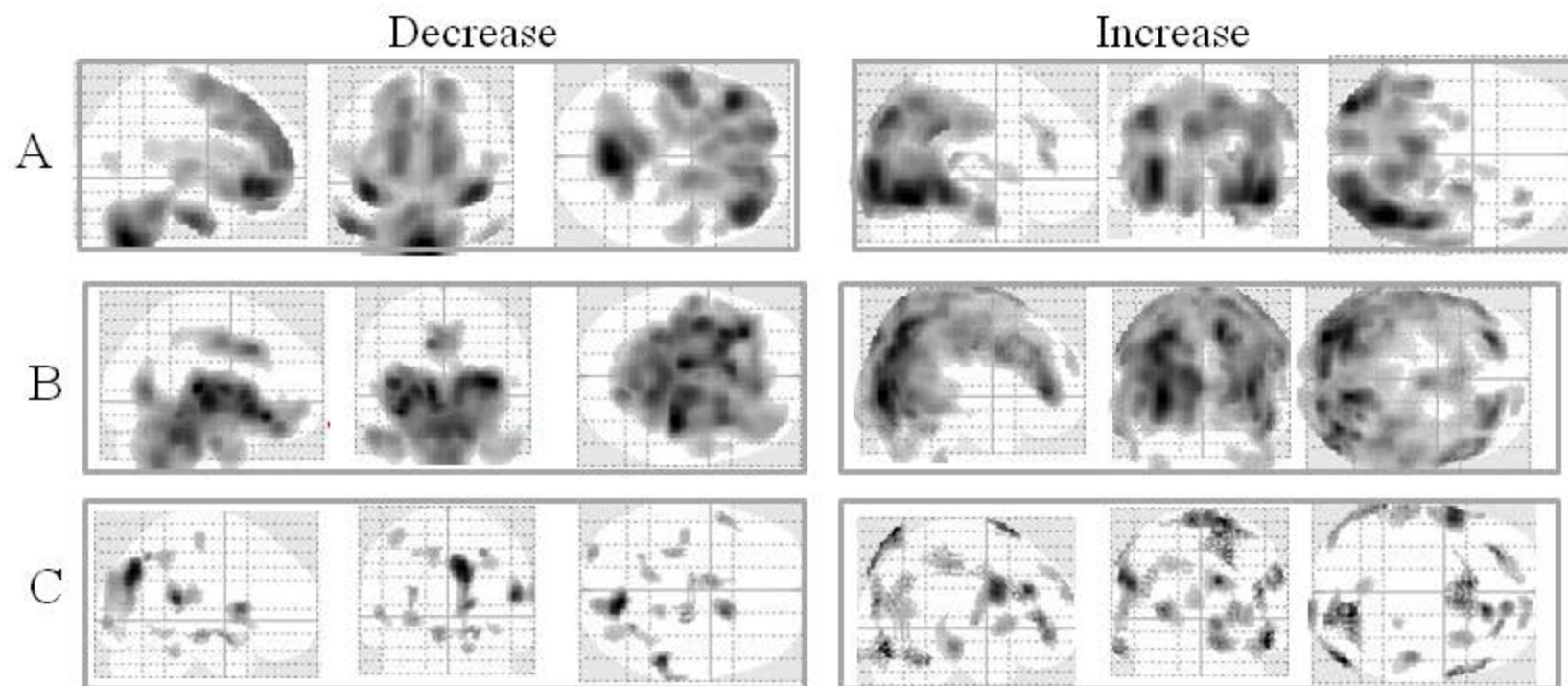
Fig.6

Table.1

| Correction | A: Central area | | B: Marginal area | |
|---|---|---|---|---|
| | Decrease | Increase | Decrease | Increase |
| IRIX data(No cor) | 1.076±0.221 | -0.772±0.135 | 0.752±0.093 | -0.979±0.166 |
| IRIX AC- data(No cor) | 1.637±0.245 | -0.461±0.113 | 0.553±0.095 | -1.530±0.223 |
| Hoffman data | 0.908±0.168 | -1.245±0.167 | 1.275±0.179 | -1.108±0.153 |
| 3D-Brain data | 1.298±0.160 | -0.953±0.104 | 0.918±0.146 | -1.332±0.191 |
| Pool data | 1.019±0.204 | -1.126±0.186 | 1.617±0.133 | -1.450±0.191 |
| Normal-SPECT data | 0.744±0.190 | -0.683±0.129 | 0.741±0.125 | -0.833±0.160 |
| ECAM Ref data | 0.774±0.218 | -0.752±0.122 | 0.770±0.118 | -0.761±0.177 |

mean±sd

Table.2

| Correction | Level2 All | Frontarl | Occipital | Temporal | Anterior | Sub-lober | Mean |
|---|---|---|---|---|---|---|---|
| IRIX data(No cor) | 0.955±0.017 | 0.949±0.025 | 0.973±0.008 | 0.953±0.012 | 0.953±0.021 | 0.944±0.023 | 0.954±0.019 |
| Hoffman data | 0.945±0.020 | 0.946±0.017 | 0.965±0.009 | 0.945±0.017 | 0.932±0.033 | 0.922±0.036 | 0.942±0.025 |
| 3D-Brain data | 0.915±0.018 | 0.921±0.023 | 0.953±0.010 | 0.919±0.020 | 0.921±0.028 | 0.903±0.028 | 0.922±0.022 |
| Pool data | 0.925±0.017 | 0.920±0.018 | 0.947±0.012 | 0.914±0.022 | 0.891±0.034 | 0.908±0.029 | 0.917±0.023 |
| Normal-SPECT data | 0.964±0.015 | 0.960±0.020 | 0.978±0.006 | 0.962±0.012 | 0.965±0.017 | 0.952±0.019 | 0.963±0.016 |
| Mean | 0.941±0.017 | 0.939±0.021 | 0.963±0.010 | 0.939±0.017 | 0.932±0.027 | 0.926±0.028 | |

mean±sd